



Targeting efflux pumps—In vitro investigations with acridone derivatives and identification of a lead molecule for MDR modulation

Palwinder Singh^{a,*}, Jatinder Kaur^a, Bhawna Yadav^b, Sneha Sudha Komath^{b,*}

^a Department of Chemistry, Guru Nanak Dev University, Amritsar 143 005, India

^b School of Life Sciences, Jawaharlal Nehru University, New Delhi 110 067, India

ARTICLE INFO

Article history:

Received 11 March 2010

Revised 30 April 2010

Accepted 1 May 2010

Available online 7 May 2010

Keywords:

Multi drug resistance

P-Glycoprotein/cdr1p/cdr2p

ATP

Mg²⁺

Acridone derivatives

Candida albicans

ABSTRACT

To search multi drug resistance modulators, acridones carrying hydroxyl amine substituent at N-10 and COOH/Cl at C-4 were investigated for their interactions with the three components of efflux pump viz. P-gp, ATP, and Mg²⁺. Experimental and theoretical results indicated that the compounds with COOH group at C-4 interact with P-gp and Mg²⁺ while other set of compounds with Cl at C-4 interact with ATP and Mg²⁺. Spot assay and R6G influx/efflux assay of compound **3** using *Candida albicans* showed decrease in the fungal growth and efflux of R6G, respectively, in presence of compound **3** suggesting the suitability of this compound for MDR modulation.

© 2010 Elsevier Ltd. All rights reserved.

1. Introduction

The practice of chemotherapy for various diseases like cancer, AIDS, malaria, bacterial and fungal infections etc. suffers from the development of resistance for the prescribed drugs. This resistance to multiple drugs (MDR)^{1,2} occurs due to the natural process of activation of ATP-binding cassette transporter proteins^{3,4} when a foreign particle enters the cell. Among various ABC transporter proteins, P-glycoprotein (P-gp) having two or more binding sites and a flip-flop mechanism of action, results in the transportation of a number of substances (including lipophilic drugs) out of the mammalian cell and causes decrease in intracellular drug concentration.⁵ Likewise cdr1p and cdr2p^{6,7} functional homologues of P-gp play vital roles in the efflux of antifungal drugs out of the cells of *Candida albicans* which might be the cause of antifungal drug resistance. Hence occurrence of MDR becomes an important issue in current medicinal chemistry due to which a combination of drugs (the modulator and the chemotherapeutic agent) are recommended for the treatment of a disease. The modulator, through its interactions with P-gp/cdr1p/cdr2p avoids the transportation of the chemotherapeutic agent out of the cell; thereby an optimum concentration of the chemotherapeutic agent could be maintained inside the cells. In this context a number of chemical entities have

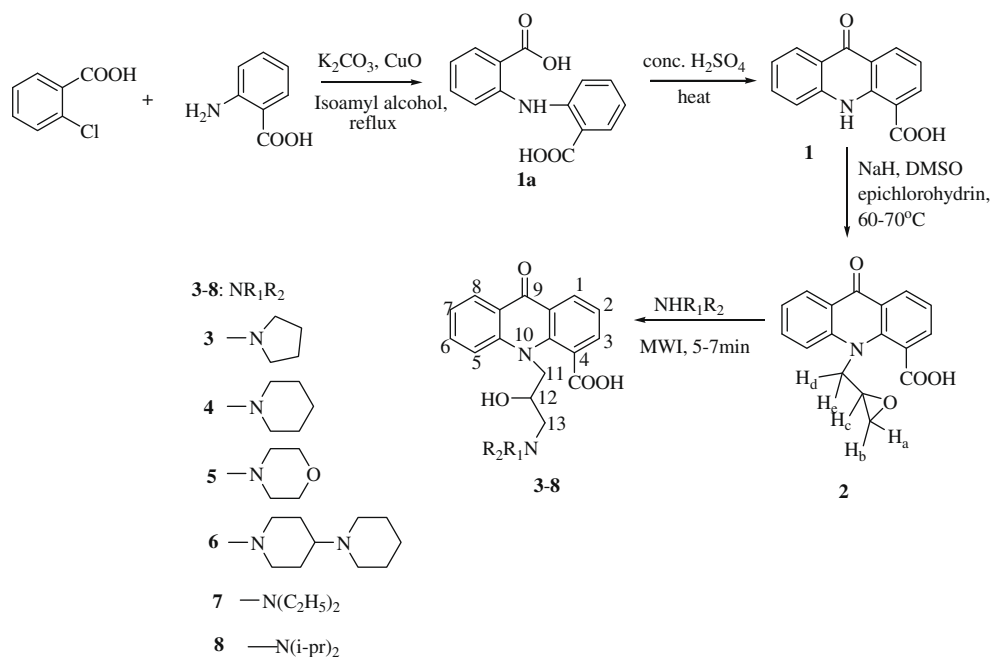
been investigated for their P-gp and cdr1p/cdr2p drug resistance modulating properties.^{8–10} Since drug transportation is an energy driven process getting energy from ATP hydrolysis, the inhibition of ATP hydrolysis could be an alternative approach for blocking the P-gp activity. ATP hydrolysis may get blocked either through interactions with ATP or by Mg²⁺ chelation.^{11–13} Therefore, the drug transporting activity of P-gp could be blocked through the interruption of components of efflux pump like P-gp, ATP, and Mg²⁺. In continuation with our earlier work¹⁴ and the importance of acridone derivatives as anti-tumor,^{15–17} anti-protozoan,^{18–20} anti-viral,²¹ and multi drug resistance (MDR) modulating^{15,22,23} agents; compounds **3–8** and **11–16** were investigated for their interactions with P-gp, ATP, and Mg²⁺. Based upon these results, some of the compounds were subjected to R6G influx/efflux assay on *C. albicans*. Compound **6** was identified as a lead for anti-candidiasis therapy²⁴ while compound **3** exhibits significant inhibition of R6G efflux from the cells of *C. albicans* and seems to be the inhibitor of cdr1p and cdr2p.

2. Results and discussion

2.1. Chemistry

Ullmann type arylation^{25–27} of anthranilic acid with *o*-chlorobenzoic acid gave **1a** which after cyclization provided the acridone skeleton (**1**) bearing –COOH group at C-4 position. Treatment of acridone **1** with NaH in DMSO followed by stirring with epichloro-

* Corresponding authors. Tel.: +91 183 2258802-09x3495; fax: +91 183 2258819.
E-mail address: palwinder_singh_2000@yahoo.com (P. Singh).



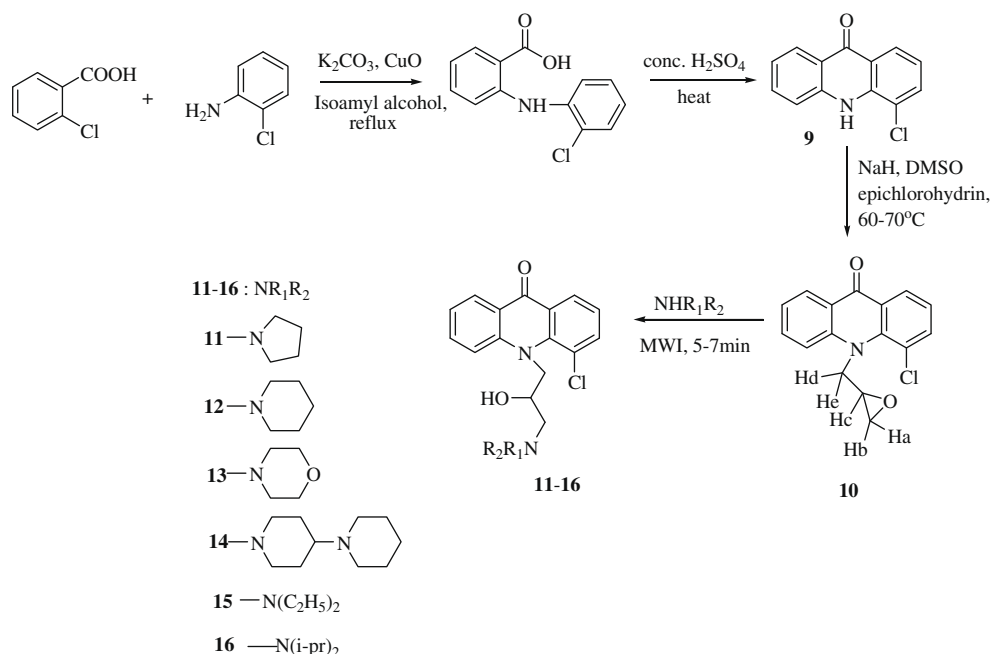
Scheme 1.

hydrin provided N-substituted acridone **2**. Irradiation of an equimolar mixture of acridone **2** and pyrrolidine in microwave oven resulted in the formation of compound **3**. Similarly, the reactions of acridone **2** with other amines under microwaves^{28,29} provided compounds **4–8** in 5–7 min (Scheme 1).

Since the acridone derivatives with COOH group at C-4 position showed better potency²⁴ in comparison to the compounds without substituent at C-4,¹⁴ further to look into the role of substituent at C-4 position, Cl was introduced through the same sequence of reactions as depicted in Scheme 1, using *o*-chloroaniline in place of anthranilic acid and compounds **11–16** (Scheme 2) were prepared.

2.2. Biology

The interactions of compounds **3–8** and **11–16** with P-gp were studied using 'Drug-P-glycoprotein Interaction' assay kit³⁰ which contains the P-gp vesicles prepared from highly resistant MDR cells, the DC-3F/ADX line. The interactions of compounds with P-gp were assessed in terms of modulation of basal activity (MgATP hydrolysis activity in the absence of drug) of P-gp measured by spectrophotometric method by continuous monitoring of ADP formation in the vesicle suspension medium. The interactions of test compound with P-gp (in the ATP binding site)/ATP/ Mg^{2+} slows down the ATPase activity of P-gp which results in the



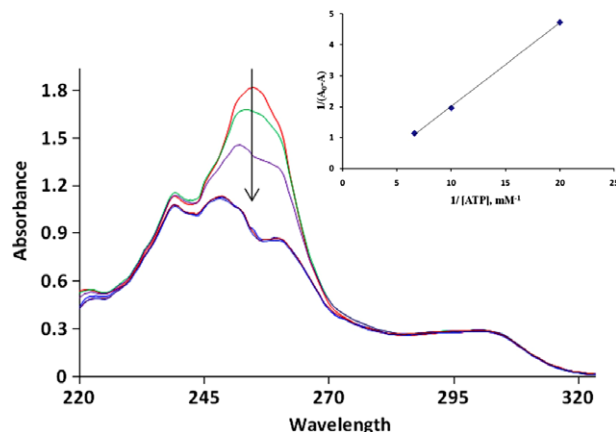
Scheme 2.

Table 1
Relative activity and percentage increase of basal activity of P-gp by compounds **3–8**

Compound	Relative activity of compd (% increase of basal activity of P-gp)		
	5 μ M	0.5 μ M	0.05 μ M
3	2.00 (100)	1.85 (85)	1.60 (60)
4	2.44 (144)	1.66 (66)	1.57 (57)
5	2.66 (166)	2.00 (100)	1.63 (63)
6	2.47 (147)	1.73 (73)	1.64 (64)
7	2.12 (112)	1.70 (70)	1.65 (65)
8	2.05 (105)	1.60 (60)	1.53 (53)
Verapamil*	2.80	2.01	1.11
Vinblastine*	1.21	1.37	0.98
Progesterone*	1.42	1.11	1.00

* Relative activity values of these compounds were taken from the booklet available with the 'Drug–P-gp interaction' assay kit.

slow conversion of phosphoenolpyruvate to pyruvate and slow formation of lactate. This will decrease the conversion of NADH to NAD⁺ and hence higher absorbance at 340 nm. Compounds were tested for their interactions with P-gp at 0.05 μ M, 0.5 μ M, and 5 μ M concentrations in triplicate. Verapamil, vinblastine and progesterone, as provided in the assay kit, were taken for comparison. The compounds under present investigations differ from each other in the nature of the cyclic tertiary base at the end of the *N*-10 substituent and presence of COOH/Cl group at C-4 of acridone ring. Compounds **3–8** exhibited more than 50% increase in the basal activity of P-gp at 0.05 μ M concentration (as per the kit manufacturer's guidelines, a 30% or more increase in the basal activity of P-gp implies the interactions of the compound with P-gp) indicating appreciable interactions with P-gp (Table 1). Compounds **5** and **6** with, respectively, morpholine and piperidino piperidine at the end of *N*-10 substituent showed better interactions with P-gp in comparison to other compounds. Looking at the various physicochemical parameters of these molecules, a variation in their partition coefficient (Log *P*) and total polar surface area (TPSA) was observed. Compound **5** with Log *P* 0.6 and TPSA 92 Å² and compound **6** with Log *P* 2.08 and TPSA 86 Å² show a difference in these two parameters from that of compounds **3**, **4**, **7**, and **8** which have Log *P* 1.16, 1.66, 1.51, 2.10, respectively, and TPSA 82.7 Å² indicating that a combination of these two parameters might be responsible for the better interactions of compounds **5** and **6** with P-gp. All the compounds with COOH group present on the acridone moiety (**3–8**) showed comparative or better interactions with P-gp than those exhibited by the reference compounds verapamil, progesterone and vinblastine. Surprisingly, none of the compounds **11–16** (with a Cl at C-4 of acridone) modulated the basal activity of P-gp pointing towards no interactions of these compounds with P-gp. In comparison to the interactions of acridones with P-gp reported earlier¹⁴ (acridones lacking COOH group), compounds **3–8** exhibited better interactions with this protein. This trend of interactions of the compounds with P-gp seems to be in parallel with their Log *P* and TPSA values (Supplementary Table S1). Among the three categories of compounds (no substituent at C-4, Cl at C-4 and COOH at C-4) compounds **3–8** have highest TPSA values and smallest (of the three categories) Log *P*, compounds **11–16** have highest Log *P* values and smaller TPSA (than compounds **3–8**) while compounds with unsubstituted C-4¹⁴ have same TPSA values as for compounds **11–16** but their Log *P* values are in between the Log *P* values of compounds **3–8** and **11–16**. Therefore, it seems that more the hydrophilicity of the compounds, better the interactions with P-gp. Therefore, a polar group like COOH is preferred on the phenyl component of acridone. This also supports the previous observation (for compounds **5** and **6**) that the Log *P* and TPSA might be the controlling parameters for the interactions of these compounds with P-gp.

**Figure 1.** Absorption spectra of compound **14** (50 μ M) on titration with 0–3 equiv of ATP in HEPES buffer. Inset: Benesi–Hildebrand plot (stoichiometry 1:1).

2.3. Interactions of compounds **3–8** and **11–16** with ATP and Mg²⁺

Looking into the second approach for modulating the drug transportation activity of P-gp via blocking of ATP hydrolysis, the interactions of acridones **3–8** and **11–16** with ATP and Mg²⁺ were investigated spectrophotometrically. UV–vis spectra of compounds **3–8** and **11–16** at 50 μ M concentration in HEPES Buffer (pH 7.2) exhibited absorption bands in the region 230–240 nm, 250–260 nm, and 385–420 nm. Addition of 0–3 equiv of ATP to 50 μ M solution of compound **14** shows that the absorption maxima at 255 nm decreases continuously and also shifts to 247 nm with a hypsochromic shift of 8 nm (Fig. 1) but further addition of ATP leads to no decrease in absorbance.

Similar trend in absorption spectra has been observed for compounds **11**, **12**, **13**, **15**, and **16**. The association constants of compounds **11–16** with ATP indicate their appreciable interactions with ATP (Table 2). Compound **14** with piperidino piperidine at the end of *N*-10 substituent exhibits significantly large association constant than the other compounds. However, no change in the absorption spectra of compounds **3–8** was observed on addition of ATP which may be due to the repulsive interactions between the carboxyl group and the phosphate group (However further investigations are needed to prove it). The Benesi–Hildebrand plot (inset of Fig. 1) and Job plot (Supplementary Fig. S1) show 1:1 stoichiometry of compound–ATP complexes. There was no change in the UV–vis spectra of compounds **11–16** on addition of adenosine, AMP and ADP indicating the selectivity of these compounds for ATP among its analogues (Fig. 2). As per the literature survey, this

Table 2

Association constants of compounds **3–8** and **11–16** with ATP and Mg²⁺ in HEPES buffer (M^{−1})

Compound	K_a (ATP) (10 ⁵)	K_a (Mg ²⁺) (10 ⁵)
3	—	1.50
4	—	19.7
5	—	3.82
6	—	1.18
7	—	7.74
8	—	2.00
11	6.57	0.95
12	5	1.48
13	4.08	17.1
14	11	18.6
15	7.9	0.39
16	1.42	2.20

—: not interacting with ATP.

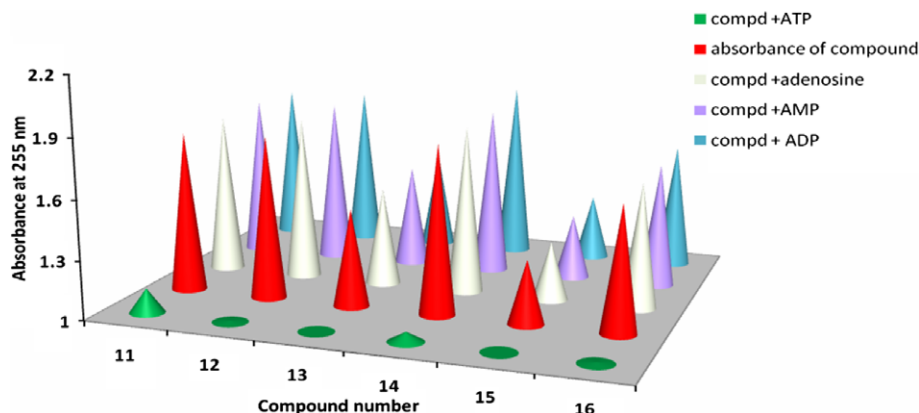


Figure 2. Absorbance change of compound **11–16** (red pyramid) at wavelength 255 nm, in the presence of ATP (green pyramid), adenosine (silver pyramid), AMP (purple pyramid), ADP (blue pyramid) indicating selectivity for ATP.

is the first report where acridone derivatives selectively bind to ATP.³¹

Since the role of Mg^{2+} in ATP hydrolysis is well established, capturing of this metal ion could slow down ATP hydrolysis and hence interruption in the supply of energy during drug effluxing. New designed acridones were investigated for their interactions with Mg^{2+} with the help of UV–vis spectral studies. Solutions of compounds **3–8** and **11–16** were prepared at 10^{-4} M concentrations in HEPES buffer (10^{-2} M) at pH 7.2 and titrated with Mg^{2+} solution ($0–0.5 \times 10^{-4}$ M). All compounds exhibited regular increase in absorbance in the region 270–310 nm, 390–415 nm and a decrease in absorbance in the region 320–340 nm with isosbestic points at 311 nm and 360 nm (Figs. 3 and 4). The association constants (Table 2) indicate significant bindings of compounds **3–8** and **11–16** with Mg^{2+} . Here also the Benesi–Hildebrand plot (inset of Figs. 3 and 4) and Job plots (Supplementary Fig. S2) indicate the 1:1 stoichiometry of compound– Mg^{2+} complexes.

Hence the present investigations have identified two sets of compounds, one which shows higher bindings with P-gp (compounds **3–8**) and second showing better interactions with ATP (compounds **11–16**) while both the sets of compounds show appreciable bindings with Mg^{2+} . The observation that both the sets of compounds (**3–8** and **11–16**) interact with Mg^{2+} led us to investigate the probable sites on the compound where Mg^{2+} binding occurs. The energy minimized structures of compounds **6** (Supplementary Fig. S3) and **14** (Supplementary Fig. S4) in presence of Mg^{2+} clearly

show that Mg^{2+} is interacting with the carbonyl oxygen of acridone and various parts of the *N*-10 substituent and there is no interaction between the C-4 substituent of acridone and metal ion.

2.4. Influx–efflux assay using *C. albicans*

Further to explore the drug influx/efflux properties of these molecules, cell based assays using *C. albicans* were carried out. Compounds **4**, **5**, and **6** have already been studied on *C. albicans* where compound **6** was causing enhanced levels of both influx and efflux of R6G due to the weakening of the cell wall of *C. albicans*.²⁴ For compounds **3** and **11–16**, first the MIC_{80} values were determined. Compound **3** had a MIC_{80} value of 781 μ g/ml while for the other compounds the values were much higher (MIC_{80} for compound **15** was 1.5 mg/ml, for rest, it was >3.0 mg/ml). So further experiments were focused on compound **3**. To look into the inhibition of *Candida* growth in presence of compound **3**, spot assays were performed. Surprisingly, there was no significant inhibition of *Candida* growth with either 0.9 mg/ml or 1 mg/ml concentration of compound **3** although some reduction in colony size is clearly visible at higher dilutions (Fig. 5). Such differences in growth of *C. albicans* between solid and liquid media are well documented.³² Due to problems of solubility in aqueous media, higher concentrations of the drug could not be tested. Next the action of compound **3** was tested in combination with cell wall perturbing agents Congo red and calcofluor white (Figs. 6 and 7,

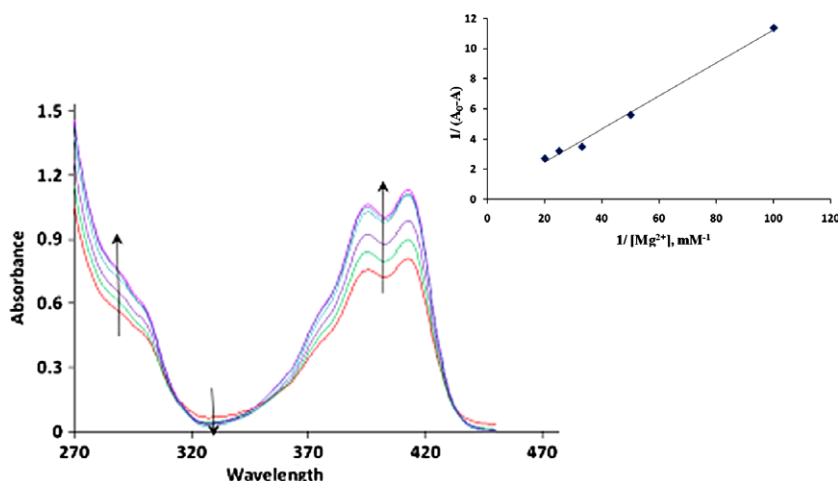


Figure 3. Absorption spectra of compound **4** in the presence of increasing concentration of Mg^{2+} (0–0.5 equiv). Arrows denote the change in absorbance in the presence of Mg^{2+} . Inset: Benesi–Hildebrand plot (stoichiometry 1:1).

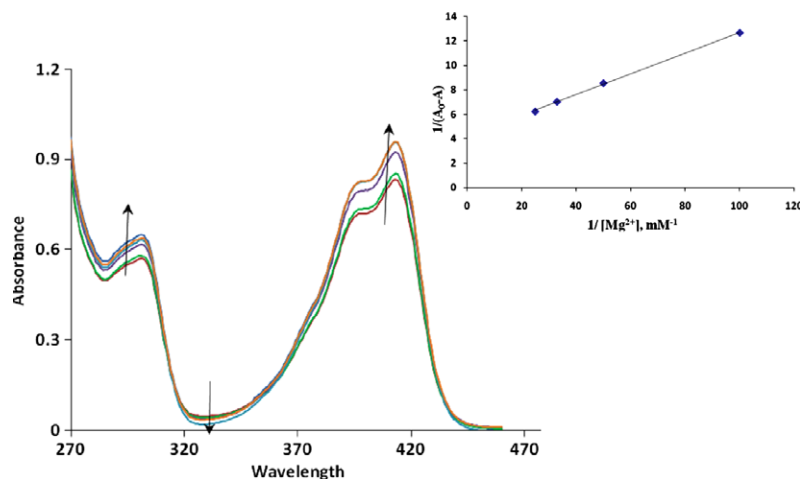


Figure 4. Absorption spectra of compound **14** in the presence of increasing concentration of Mg^{2+} (0–0.5 equiv). Arrows denote the change in absorbance in the presence of Mg^{2+} . Inset: Benesi–Hildebrand plot (stoichiometry 1:1).

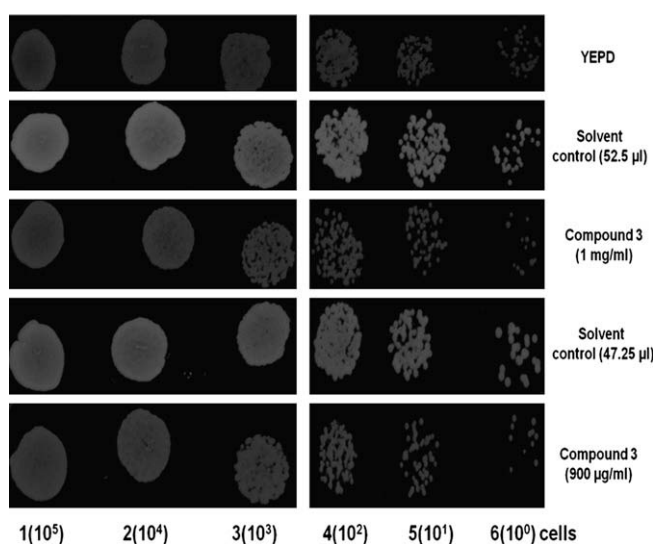


Figure 5. Plate assay in the presence of compound **3**. Details are given under methods. Spot numbers along with cell dilutions in parenthesis.

respectively). No significant effect was seen in either of these combinations, clearly indicating that compound **3** did not influence the integrity of the cell wall of the organism. Since it appeared from the MIC_{80} values that compound **3** was toxic to *Candida* cells, we next looked to see if it would in any way influence the drug efflux pumps in the organism. For this, spot assays were carried in the presence of a combination of compound **3** and rhodamine 6G (R6G), which is also a substrate for both *cdr1p* and *cdr2p* in *C. albicans*. It was found that a combination of compound **3** and R6G in the growth medium inhibited the cell growth (Fig. 8). These results could suggest that either compound **3** is facilitating the entry of R6G inside the cells, or it is somehow negatively affecting the efflux of R6G from the cells.

To investigate this further, R6G influx–efflux assays were done in the presence of compound **3**, to see if there was any change in the influx or efflux levels of R6G in the presence of this compound. Influx and efflux of R6G was monitored in the *Candida* cells in the absence and the presence (800 $\mu\text{g}/\text{ml}$) of compound **3**. A solvent control set was also assayed to account for the action of the solvent on this process. Within limits of experimental error, the influx data suggests that, the presence of compound **3** increases the rate of

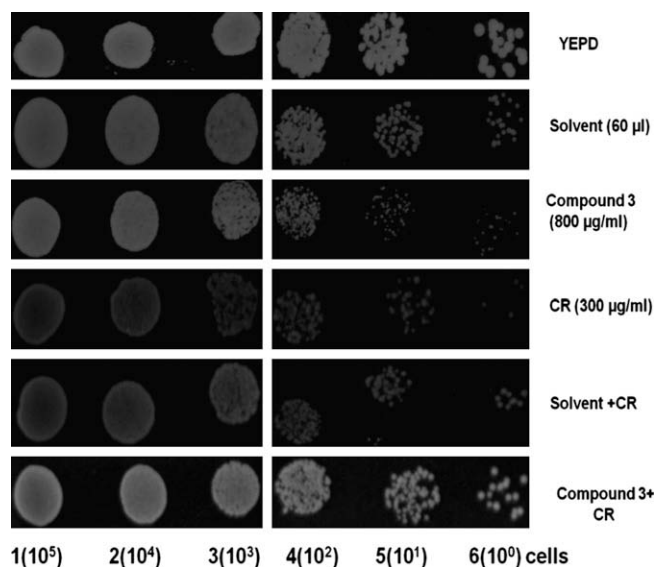


Figure 6. Plate assay in the presence of a combination of compound **3** and Congo red. Details are given under methods. Spot numbers along with cell dilutions in parenthesis.

R6G influx inside the cells (Fig. 9). However, it may be pointed out that the total amount of R6G in the cells is roughly the same at the end of 3 h, indicating that the toxicity of the combination of compound **3** with R6G cannot be due to enhanced levels of the toxin entering the cell. In the absence of glucose the efflux of R6G was the same for all sets and was far less than in the presence of glucose, indicating that (i) the presence of compound **3** did not significantly perturb the cell wall of the organism and lead to higher levels of passive efflux from the cells and (ii) the efflux of R6G was primarily due to an active process. The efflux data in the presence of glucose suggests that in the presence of compound **3** the level of R6G efflux from the cells is less than the control set. On comparison with the solvent control, it was observed that the efflux in the presence of the compound was inhibited more relative to the solvent control up to a period of 60 min (Fig. 10). It may be pointed out, however, that at higher time points, the solvent itself appeared to influence the efflux of R6G from the cells, indicating that the cells were probably being affected by the organic solvent present in the assay buffer.

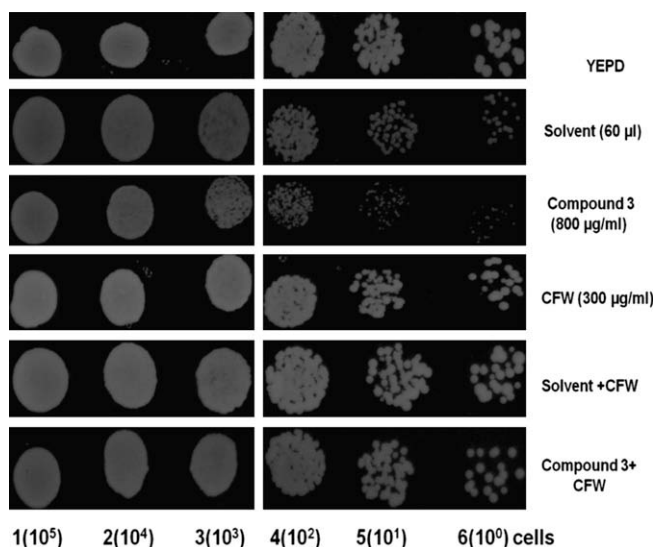


Figure 7. Plate assay in the presence of a combination of compound **3** and calcofluor white.

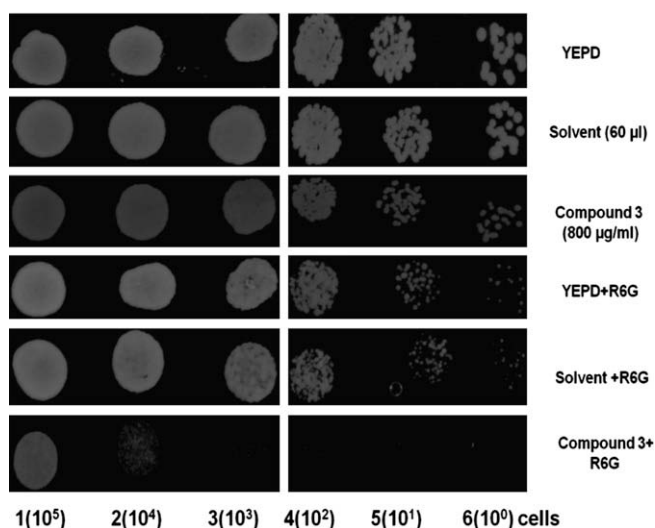


Figure 8. Plate assay in the presence of a combination of compound **3** and rhodamine 6G.

2.5. Docking studies

Since a difference in the behavior of compounds **3–8** and **11–16** for interactions with P-gp was observed in ‘Drug–P-glycoprotein Interaction Assay’, it was planned to perform the docking of these two categories of compounds in the ATP and drug binding sites of P-gp. Compounds **3–8** and **11–16** were built using the builder toolkit of the software package ArgusLab 4.0.1³³ and energy minimized using semi-empirical quantum mechanical method PM3. The crystal coordinates of the P-glycoprotein (pdb ID 1MV5, pdb ID 3G60)⁵ were downloaded from protein data bank. For the docking of compounds **3–8** and **11–16**, a volume of 15 Å³ was taken around ADP in case of 1MV5 crystal coordinates representing the ATP binding site and 15 Å³ around hexapeptide in case of 3G60 crystal coordinates representing drug binding site. Mg²⁺ is also visible in the ATP binding site of P-gp. For the docking process, the energy minimized molecule was pasted on the protein. The docking program implements an efficient grid based docking algorithm which approximates an exhaustive search within the free volume of the

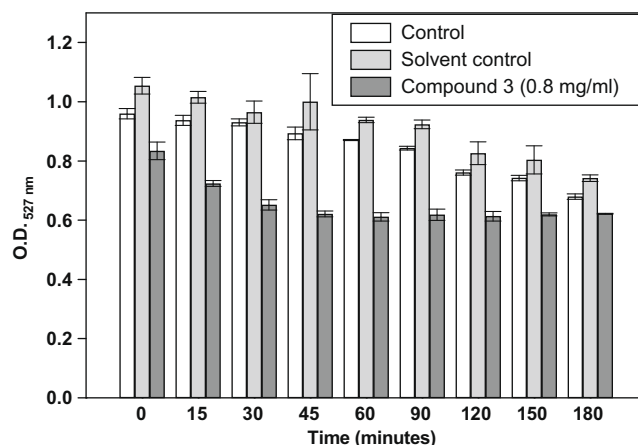


Figure 9. R6G influx in CA14 cells in the presence of compound **3**. A higher O.D._{527 nm} indicates higher levels of R6G in the buffer and hence a lower influx inside the cells.

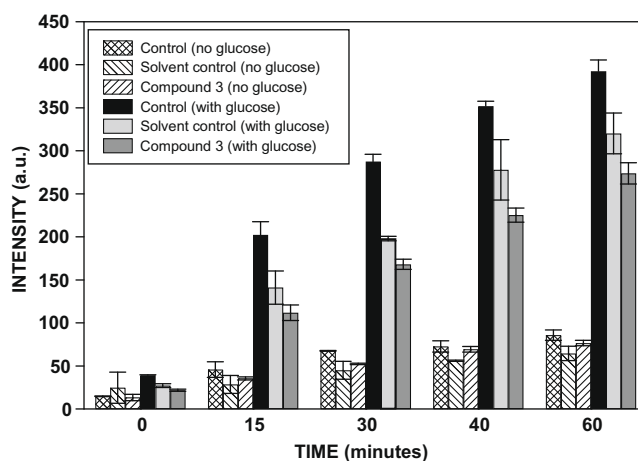


Figure 10. R6G efflux from CA14 cells in the presence of compound **3**. A higher intensity level indicates higher levels of R6G in buffer and hence a higher value of R6G influx from the cells.

binding site cavity. Thus, docking occurs between the flexible ligand parts of the compound and enzyme. The ligand orientation was determined by a shape scoring function based on Ascore and the final positions were ranked by lowest interaction energy values.

Docking of compounds **3–8** in the ATP binding site of P-gp indicate appreciable interactions between these compounds and the amino acids of P-gp. Compound **3** on docking in the ATP binding site of P-gp exhibited H-bond interaction from its carbonyl oxygen with Y1393, OH group with D1353 and COOH group with D1353 and Y1352 residues (Fig. 11). Docking of compound **4** in the ATP binding site of P-gp also indicated H-bond interactions between the carbonyl oxygen of acridone moiety, OH group of hydroxyl amine chain with Y1393 and D1353 residues. Compound **5** on docking in the ATP binding site showed interactions between carbonyl oxygen and OH of carboxyl group with Y1352, Y1393, and D468, respectively. Docking of compound **6** in the ATP binding site of P-gp showed interactions through nitrogen of piperidino piperidine moiety, OH of hydroxyl amine chain and OH of carboxyl group with Y2393, Y1393, V479, and E473, respectively. The H-bond interaction between the nitrogen of piperidino piperidine moiety of compound **6** and Y2393 (which is not observed with other amines) indicates that a large group (which could extend

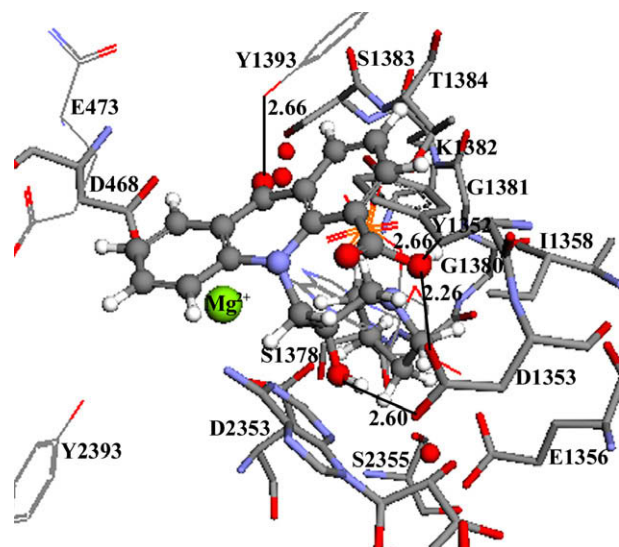


Figure 11. Compound **3** docked in the ATP binding site of P-gp. Hs' are omitted for clarity.

towards Y2393) with H-donor/acceptor sites is desirable at the end of *N*-10 substituent. Compounds **7** and **8** also exhibit similar interactions in the ATP binding site of P-gp.

Docking of compounds **3–8** in the drug binding site of P-gp indicate that these compounds show less interactions with the amino acids here in comparison to their interactions in the ATP binding site (Table 3), supporting the experimental observation (P-gp–drug interaction assay). However, compounds **11–16** did not enter either the ATP binding site or drug binding site during the docking of these compounds in the respective crystal coordinates of the protein. Therefore, the docking studies support the experimental observations of appreciable interactions of compounds **3–8** and no interactions of compounds **11–16** with P-gp and also indicate the preference of compounds **3–8** for the ATP binding site over the drug binding site of P-gp.

3. Conclusions

1. 'Drug–P-gp interaction' experiment showed that compounds **3–8** exhibit significant interactions with P-gp while compounds **11–16** did not interact with P-gp which is also supported by docking studies. Log *P* and TPSA values of these compounds

Table 3

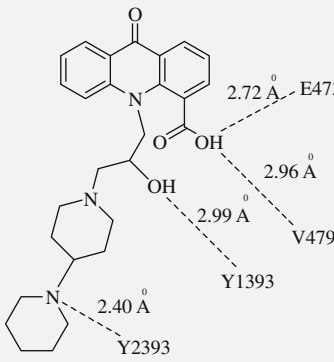
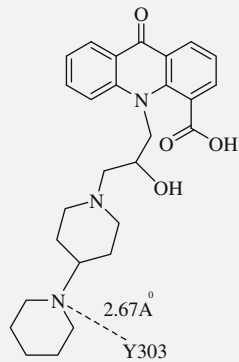
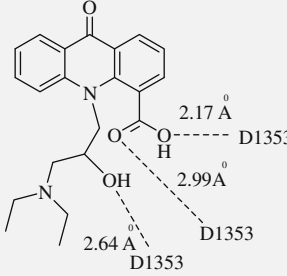
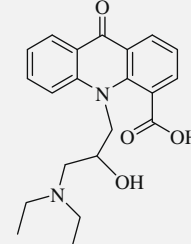
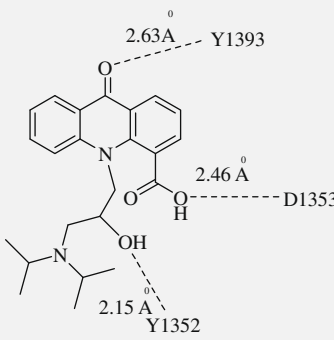
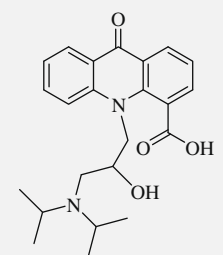
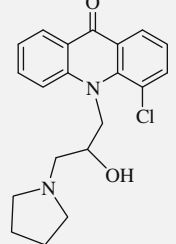
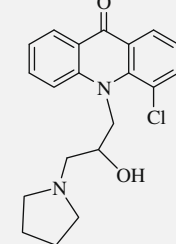
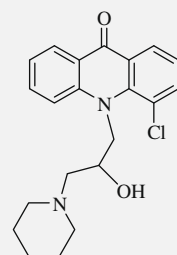
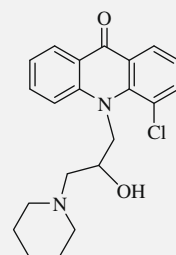
Comparison of interactions of compounds in the ATP binding site and the drug binding site of P-gp. H-bond distances are given in Å

Compound	Interactions in ATP binding site	Interactions in drug binding site
3		
4		
5		

No H-bond Interactions

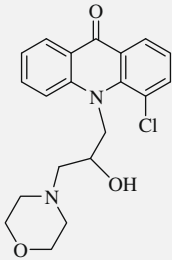
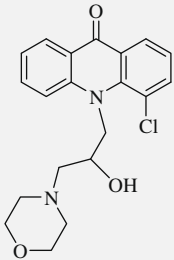
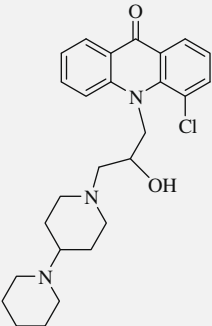
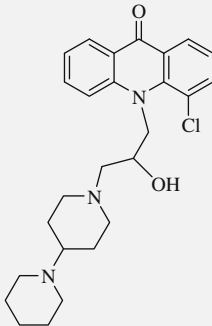
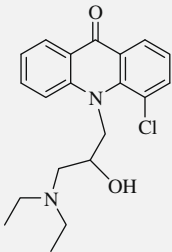
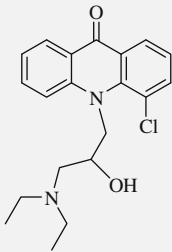
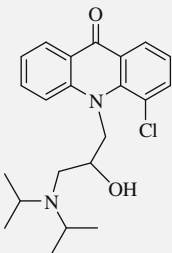
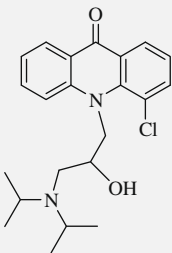
No H-bond Interactions

Table 3 (continued)

Compound	Interactions in ATP binding site	Interactions in drug binding site
6		
7		 <p>No H-bond Interactions</p>
8		 <p>No H-bond Interactions</p>
11	 <p>No H-bond Interactions</p>	 <p>No H-bond Interactions</p>
12	 <p>No H-bond Interactions</p>	 <p>No H-bond Interactions</p>

(continued on next page)

Table 3 (continued)

Compound	Interactions in ATP binding site	Interactions in drug binding site
13	 <p>No H-bond Interactions</p>	 <p>No H-bond Interactions</p>
14	 <p>No H-bond Interactions</p>	 <p>No H-bond Interactions</p>
15	 <p>No H-bond Interactions</p>	 <p>No H-bond Interactions</p>
16	 <p>No H-bond Interactions</p>	 <p>No H-bond Interactions</p>

indicate that the hydrophilicity might be the controlling parameter for their interactions with P-gp since more hydrophilic compounds (**3–8**) exhibit better interactions with P-gp.

- On the basis of UV–vis spectral studies, irrespective of the nature of C-4 substituent, appreciable interactions were observed between compounds **3–8**, **11–16** with Mg^{2+} indicating that Mg^{2+} might be interacting at sites other than the C-4 substituent (probably OH and N present at N-10 substituent, as shown by the energy minimized structures of compound– Mg^{2+} complex). Only compounds **11–16** interact with ATP and the non-interactions of compounds **3–8** with ATP seems to be due to the repulsion between carboxyl group and phosphate group.

- Influx–efflux assay on *C. albicans* indicate that the presence of compound **3** decreases the efflux of R6G from the *Candida* cells which might be occurring through the inhibition of cdr1p/cdr2p transporting proteins. Compound **3** is suitable candidate for further investigations for MDR modulating properties.

4. Experimental

4.1. General note

Melting points were determined in capillaries and are uncorrected. 1H and ^{13}C NMR spectra were recorded on JEOL 300 MHz and 75 MHz NMR spectrometer, respectively, using $CDCl_3$ as solvent.

Chemical shifts are given in ppm with TMS as an internal reference. J values are given in Hertz. IR and UV spectral data were recorded on FTIR 8400S Shimadzu and BioTek PowerWave XS instruments, respectively. The reactions corresponding to epoxy ring opening with amines were performed in domestic microwave oven (INALSA model 1MW17EG) with microwave power 700 W and operating frequency 2450 MHz. Reactions were monitored by thin layer chromatography (TLC) on glass plates coated with Silica Gel GF-254. Column chromatography was performed with 100–200 mesh silica. In ^{13}C NMR spectral data, +ve, –ve terms correspond to CH_3 , CH, and CH_2 signals, respectively, in DEPT-135 NMR spectra.

4.2. General procedure for the syntheses of compounds 1 and 9 (procedure A)²²

A mixture of 2-chlorobenzoic acid (1.56 g, 10 mmol), anthranilic acid/*o*-chloroaniline (10 mmol), powdered CuO (25 mg) and K_2CO_3 (1.5 g, ~11 mmol) in isoamyl alcohol (10 ml) was heated at 160 °C for 10 h. After cooling, the alcohol was evaporated under vacuum and the residue was dissolved in hot water (120 ml) and acidified with 10 N HCl. The precipitates were filtered and washed with hot water. The solid product was dissolved in ethyl acetate, the solution was dried over anhydrous Na_2SO_4 and evaporated to dryness. The crude product was purified by column chromatography over silica gel using a mixture of ethyl acetate and hexane (1:1) as the eluent. This product was taken in concd H_2SO_4 (just to dissolve the compound) and heated on water bath for 1.5 h. Reaction mixture was added to hot water and the resulting precipitates were filtered to get acridone **1** and **9**.

4.3. General procedure for the syntheses of compounds 2 and 10 (procedure B)

Sodium hydride (3.0 mmol) was washed with dry hexane and taken in 15 ml of dimethyl sulphoxide. To this solution, acridone **1/9** (2.5 mmol) and epichlorohydrin (3.0 mmol) were added and the reaction mixture was stirred for 17–18 h at 70–80 °C (TLC monitoring). The reaction mixture was extracted with ethyl acetate. The organic phase was dried over anhydrous Na_2SO_4 . The solvent was distilled off and the residue was column chromatographed using ethyl acetate and hexane (7:1) as eluents to isolate pure compound **2**²⁴ and **10**.

4.3.1. 4-Chloro-10-((oxiran-2-yl)methyl)acridin-9(10H)-one (10)

Compound **10** (0.84 g, 2.95 mmol) was synthesized using compound **9** (1 g, 4.36 mmol) according to the synthetic procedure B as a yellow solid in a yield of 68%, mp 130 °C; IR (KBr, cm^{-1}): 1635 ($\text{C}=\text{O}$); UV (ethanol + HEPES buffer) λ_{max} (ϵ) 231 (8870), 246 (21,560), 404 (11,090); ^1H NMR (300 MHz, CDCl_3) δ 2.68 (dd, 1H, $^2J = 2.7$ Hz, $^3J = 2.4$ Hz, H_b), 2.93 (dd, 1H, $^2J = 3.39$ Hz, $^3J = 4.8$ Hz, H_a), 3.48–3.50 (m, 1H, H_c), 4.39 (dd, 1H, $^2J = 16.9$ Hz, $^3J = 4.6$ Hz, H_e), 4.85 (dd, 1H, $^2J = 16.9$ Hz, $^3J = 1.9$ Hz, H_d), 7.26–7.32 (m, 2H, ArH), 7.56–7.74 (m, 3H, ArH), 8.53 (dd, 2H, $^2J = 8.1$ Hz, $^3J = 1.5$ Hz, ArH); ^{13}C (Normal/DEPT-135) δ 45.03 (–ve, CH_2), 47.55 (–ve, CH_2), 50.23 (+ve, CH), 115.10 (+ve, ArCH), 122.69 (+ve, ArCH), 122.42 (absent, ArC), 127.78 (+ve, ArCH), 133.95 (+ve, ArCH), 142.51 (+ve, ArCH), 178.05 ($\text{C}=\text{O}$), MS (FAB) 285, 287 (3:1) (M^+). Anal. Calcd for $\text{C}_{17}\text{H}_{13}\text{NO}_4$: C, 67.26; H, 4.23; N, 4.90. Found: C, 67.24; H, 4.25; N, 4.87.

4.4. General procedure for the syntheses of compounds 3–8 and 11–16 (procedure C)

A mixture of acridone **2** (1 mmol) and appropriate amine (1 mmol) was irradiated in microwave oven for 5–7 min. On completion of the reaction (TLC), it was washed with diethyl ether to

isolate pure product. Spectral data for compounds **3–6** has already been reported.²⁴

4.4.1. 10-(3-Diethylamino-2-hydroxy-propyl)-9-oxo-9,10-dihydro-acridine-4-carboxylic acid (7)

Compound **7** (0.08 g, 0.23 mmol) was synthesized using compound **2** (0.1 g, 0.34 mmol) according to the synthetic procedure C as a yellow solid in a yield of 67%, mp 115 °C; IR (KBr, cm^{-1}): 1610 ($\text{C}=\text{O}$), 1680 ($\text{C}=\text{O}$), 3250 (OH), 3360 (OH); UV (ethanol + HEPES buffer) λ_{max} (ϵ) 232 (9880), 256 (25,530), 412 (6040); ^1H NMR (300 MHz, CDCl_3) 1.25–1.40 (m, 6H, $2 \times \text{CH}_3$), 3.20–3.53 (m, 6H, $13\text{-H} + 2 \times \text{NCH}_2$), 4.67–4.92 (m, 3H, $12\text{-H} + 11\text{-H}$), 7.26–7.40 (m, 2H, ArH), 7.42–7.46 (m, 3H, ArH), 8.35–8.64 (m, 2H, ArH), 12.09 (br s, 1H, COOH); ^{13}C NMR (normal/DEPT-135) δ 12.02 (+ve, CH_3), 47.75 (–ve, CH_2), 50.20 (–ve, CH_2), 57.64 (–ve, CH_2), 66.36 (+ve, C-12), 115.80 (absent, ArC), 121.48 (+ve, ArCH), 122.55 (+ve, ArCH), 127.64 (+ve, ArCH), 128.42 (+ve, ArCH), 133.90 (+ve, ArCH), 167.12 ($\text{C}=\text{O}$), 178.52 ($\text{C}=\text{O}$), MS (FAB) 369 ($\text{M}^+ + 1$). Anal. Calcd for $\text{C}_{21}\text{H}_{24}\text{N}_2\text{O}_4$: C, 68.46; H, 6.57; N, 7.60. Found: C, 68.48; H, 6.55; N, 7.65.

4.4.2. 10-(3-Diisopropylamino-2-hydroxy-propyl)-9-oxo-9,10-dihydro-acridine-4-carboxylic acid (8)

Compound **8** (0.08 g, 0.21 mmol) was synthesized using compound **2** (0.1 g, 0.34 mmol) according to the synthetic procedure C as a light yellow solid in a yield of 62%, mp 120 °C; IR (KBr, cm^{-1}): 1605 ($\text{C}=\text{O}$), 1685 ($\text{C}=\text{O}$), 3220 (OH); 3380 (OH); UV (ethanol + HEPES buffer) λ_{max} (ϵ) 232 (10,050), 253 (26,780), 412 (6430); ^1H NMR (300 MHz, CDCl_3) δ 1.56 (d, $J = 6.6$ Hz, 12H, $4 \times \text{CH}_3$), 3.13–3.18 (m, 1H, NCH), 3.71–3.73 (m, 3H, $13\text{-H} + \text{NCH}$), 4.46–4.55 (m, 3H, $11\text{-H} + 12\text{-H}$), 7.21–7.36 (m, 3H, ArH), 7.68–7.69 (m, 2H, ArH), 8.35–8.73 (m, 2H, ArH), 11.51 (br s, 1H, COOH); ^{13}C NMR (normal/DEPT-135) δ 19.35 (+ve, CH_3), 21.44 (+ve, CH_3), 45.05 (–ve, CH_2), 47.59 (–ve, CH_2), 49.41 (+ve, CH), 50.42 (+ve, CH), 66.26 (+ve, C-12), 115.36 (absent, ArC), 121.74 (+ve, ArCH), 122.43 (+ve, ArCH), 127.85 (+ve, ArCH), 133.78 (+ve, ArCH), 134.00 (+ve, ArCH), 167.35 ($\text{C}=\text{O}$), 178.08 ($\text{C}=\text{O}$); MS (FAB) 397 ($\text{M}^+ + 1$). Anal. Calcd for $\text{C}_{23}\text{H}_{28}\text{N}_2\text{O}_4$: C, 69.67; H, 7.12; N, 7.07. Found: C, 69.65; H, 7.16; N, 7.09.

4.4.3. 4-Chloro-10-(2-hydroxy-3-(pyrrolidin-1-yl)propyl)acridin-9(10H)-one (11)

Compound **11** (0.08 g, 0.24 mmol) was synthesized using compound **10** (0.1 g, 0.35 mmol) according to the synthetic procedure C as a yellow solid in a yield of 68%, mp 105 °C; IR (KBr, cm^{-1}): 1595 ($\text{C}=\text{O}$), 3355 (OH); UV (ethanol + HEPES buffer) λ_{max} (ϵ) 235 (10,320), 256 (22,600), 413 (5150); ^1H NMR (300 MHz, CDCl_3) δ 1.79–1.84 (m, 4H, $2 \times \text{CH}_2$ pyrrol), 2.58–2.66 (m, 3H, 1H of $13\text{-H} + 2\text{H}$ of NCH_2), 2.75 (dd, 2H, $^2J = 6.7$ Hz, $^3J = 2.2$ Hz, NCH_2), 2.78 (dd, 1H, $^2J = 11.8$ Hz, $^3J = 9.7$ Hz, 1H of 13-H), 4.29–4.32 (m, 1H, 12-H), 4.45 (dd, 1H, $^2J = 16.2$ Hz, $^3J = 4.2$ Hz, 11-H), 4.57 (dd, 1H, $^2J = 16.0$ Hz, $^3J = 7.05$ Hz, 11-H), 7.29 (dd, 2H, $^2J = 8.1$ Hz, $^3J = 4.2$ Hz, ArH), 7.71 (dd, 3H, $^2J = 4.2$ Hz, $^3J = 0.9$ Hz, ArH), 8.53 (t, 1H, $J = 1.2$ Hz, ArH), 8.56 (t, 1H, $J = 1.2$ Hz, ArH); ^{13}C NMR (normal/DEPT-135) δ 23.82 (–ve, CH_2), 50.09 (–ve, CH_2), 54.00 (–ve, CH_2), 59.76 (–ve, CH_2), 67.77 (+ve, C-12), 115.33 (+ve, ArCH), 121.38 (+ve, ArCH), 122.37 (absent, ArC), 122.75 (+ve, ArCH), 127.73 (+ve, ArCH), 133.69 (+ve, ArCH), 177.88 ($\text{C}=\text{O}$); MS (FAB) 356, 358 (3:1) (M^+). Anal. Calcd for $\text{C}_{20}\text{H}_{21}\text{ClN}_2\text{O}_2$: C, 67.32; H, 5.93; N, 7.85. Found: C, 67.34; H, 5.99; N, 7.88.

4.4.4. 4-Chloro-10-(2-hydroxy-3-(piperidin-1-yl)propyl)acridin-9(10H)-one (12)

Compound **12** (0.08 g, 0.22 mmol) was synthesized using compound **10** (0.1 g, 0.35 mmol) according to the synthetic procedure C as a yellow solid in a yield of 63%, mp 110 °C; IR (KBr, cm^{-1}):

1585 (C=O), 3354 (OH); UV (ethanol + HEPES buffer) λ_{max} (ϵ) 233 (10,810), 252 (24,850), 404 (7110); ^1H NMR (300 MHz, CDCl_3) δ 1.63 (br s, 6H, $3 \times \text{CH}_2$), 2.51–2.62 (m, 6H, $3 \times \text{NCH}_2$), 4.30–4.40 (m, 1H, 12-H), 4.44 (dd, 1H, $^2J = 16.2$ Hz, $^3J = 3.6$ Hz, 11-H), 4.55 (dd, 1H, $^2J = 16.0$ Hz, $^3J = 7.0$ Hz, 11-H), 7.23–7.29 (m, 2H, ArH), 7.70–7.73 (m, 3H, ArH), 8.49 (t, 1H, $J = 1.2$ Hz, ArH), 8.52 (t, 1H, $J = 1.0$ Hz, ArH); ^{13}C NMR (normal/DEPT-135) δ 25.86 (–ve, CH_2), 50.24 (–ve, CH_2), 54.74 (–ve, CH_2), 62.36 (–ve, CH_2), 65.98 (+ve, C-12), 115.41 (+ve, ArCH), 117.30 (+ve, ArCH), 119.52 (+ve, ArCH), 121.34 (absent, ArC), 127.66 (+ve, ArCH), 133.66 (+ve, ArCH), 178.53 (C=O), MS (FAB) 370, 372 (3:1) (M^+). Anal. Calcd for $\text{C}_{21}\text{H}_{23}\text{ClN}_2\text{O}_2$: C, 68.01; H, 6.25; N, 7.55. Found: C, 68.06; H, 6.28; N, 7.57.

4.4.5. 4-Chloro-10-(2-hydroxy-3-morpholinopropyl)acridin-9(10H)-one (13)

Compound **13** (0.08 g, 0.22 mmol) was synthesized using compound **10** (0.1 g, 0.35 mmol) according to the synthetic procedure C as a yellow solid in a yield of 63%, mp 120 °C; IR (KBr, cm^{-1}): 1592 (C=O), 3343 (OH); UV (ethanol + HEPES buffer) λ_{max} (ϵ) 235 (16,670), 252 (27,860), 413 (8040); ^1H NMR (300 MHz, CDCl_3) δ 2.53–2.64 (m, 2H, 13-H), 2.66–2.71 (m, 4H, $2 \times \text{NCH}_2$), 3.75 (t, 4H, $J = 4.5$ Hz, $2 \times \text{OCH}_2$), 4.33–4.42 (m, 1H, 12-H), 4.48 (dd, 1H, $^2J = 16.2$ Hz, $^3J = 3.6$ Hz, 11-H), 4.58 (dd, 1H, $^2J = 16.0$ Hz, $^3J = 7.2$ Hz, 11-H), 7.19–7.26 (m, 2H, ArH), 7.65–7.70 (m, 3H, ArH), 8.42 (t, 1H, $J = 0.9$ Hz, ArH), 8.45 (t, 1H, $J = 1.2$ Hz, ArH); ^{13}C NMR (normal/DEPT-135) δ 50.16 (–ve, CH_2), 53.85 (–ve, CH_2), 62.33 (–ve, CH_2), 66.10 (–ve, CH_2), 66.92 (+ve, C-12), 115.37 (+ve, ArCH), 119.21 (+ve, ArCH), 120.23 (+ve, ArCH), 121.43 (absent, ArC), 127.70 (+ve, ArCH), 133.71 (+ve, ArCH), 177.65 (C=O), MS (FAB) 372, 374 (3:1) (M^+). Anal. Calcd for $\text{C}_{20}\text{H}_{21}\text{ClN}_2\text{O}_3$: C, 64.43; H, 5.68; N, 7.51. Found: C, 64.45; H, 5.71; N, 7.55.

4.4.6. 4-Chloro-10-(2-hydroxy-3-(4-(piperidin-1-yl)piperidin-1-yl)propyl)acridin-9(10H)-one (14)

Compound **14** (0.10 g, 0.23 mmol) was synthesized using compound **10** (0.1 g, 0.35 mmol) according to the synthetic procedure C as a yellow solid in a yield of 65%, mp 115 °C; IR (KBr, cm^{-1}): 1590 (C=O), 3345 (OH); UV (ethanol + HEPES buffer) λ_{max} (ϵ) 236 (11,720), 254 (29,680), 407 (7520); ^1H NMR (300 MHz, CDCl_3) δ 1.45–1.60 (m, 2H, CH_2), 1.74–1.75 (m, 8H, $4 \times \text{CH}_2$), 1.98–2.25 (m, 1H, CH), 2.28–2.48 (m, 2H, NCH_2), 2.50–2.58 (m, 6H, $3 \times \text{NCH}_2$), 2.95–2.98 (m, 2H, 13-H), 4.27–4.32 (m, 1H, 12-H), 4.42 (dd, 1H, $^2J = 16.2$ Hz, $^3J = 3.3$ Hz, 11-H), 4.55 (dd, 1H, $^2J = 15.9$ Hz, $^3J = 7.2$ Hz, 11-H), 7.24–7.29 (m, 1H, ArH), 7.69–7.71 (m, 4H, ArH), 8.50 (t, 1H, $J = 1.0$ Hz, ArH), 8.53 (t, 1H, $J = 0.9$ Hz, ArH); ^{13}C NMR (normal/DEPT-135) δ 24.83 (–ve, CH_2), 26.42 (–ve, CH_2), 50.28 (–ve, CH_2), 52.66 (–ve, CH_2), 55.30 (–ve, CH_2), 61.49 (–ve, CH_2), 62.15 (+ve, CH), 66.50 (+ve, C-12), 115.56 (+ve, ArCH), 119.25 (+ve, ArCH), 121.11 (+ve, ArCH), 121.23 (+ve, ArCH), 127.69 (absent, ArC), 133.62 (+ve, ArCH), 177.00 (C=O); MS (FAB) 453, 455 (3:1) (M^+). Anal. Calcd for $\text{C}_{26}\text{H}_{32}\text{ClN}_3\text{O}_2$: C, 68.78; H, 7.10; N, 9.26. Found: C, 68.81; H, 7.16; N, 9.29.

4.4.7. 4-Chloro-10-(3-(diethylamino)-2-hydroxypropyl)acridin-9(10H)-one (15)

Compound **15** (0.08 g, 0.22 mmol) was synthesized using compound **10** (0.1 g, 0.35 mmol) according to the synthetic procedure C as a yellow solid in a yield of 64%, mp 120 °C; IR (KBr, cm^{-1}): 1595 (C=O), 3345 (OH); UV (ethanol + HEPES buffer) λ_{max} (ϵ) 234 (10,560), 253 (22,770), 405 (6600); ^1H NMR (300 MHz, CDCl_3) δ 1.06 (t, 6H, $J = 7.3$ Hz, $2 \times \text{CH}_3$), 2.54–2.74 (m, 6H, 13-H + $2 \times \text{NCH}_2$), 4.20–4.28 (m, 1H, 12-H), 4.42 (dd, 1H, $^2J = 15.9$ Hz, $^3J = 3.3$ Hz, 11-H), 4.54 (dd, 1H, $^2J = 16.05$ Hz, $^3J = 7.35$ Hz, 11-H), 7.25–7.27 (m, 2H, ArH), 7.70–7.72 (m, 3H, ArH), 8.48 (t, 1H, $J = 1.0$ Hz, ArH), 8.51 (t, 1H, $J = 0.3$ Hz, ArH); ^{13}C NMR (normal/DEPT-135) δ 11.82 (+ve, CH_3), 47.56 (–ve, CH_2), 50.20 (–ve, CH_2),

57.35 (–ve, CH_2), 66.45 (+ve, C-12), 115.70 (+ve, ArCH), 121.48 (+ve, ArCH), 122.36 (absent, ArC), 127.54 (+ve, ArCH), 128.04 (+ve, ArCH), 133.90 (+ve, ArCH), 178.52 (C=O), MS (FAB) 358, 360 (3:1) (M^+). Anal. Calcd for $\text{C}_{20}\text{H}_{23}\text{ClN}_2\text{O}_2$: C, 66.94; H, 6.46; N, 7.81. Found: C, 66.98; H, 6.47; N, 7.86.

4.4.8. 4-Chloro-10-(3-(diisopropylamino)-2-hydroxypropyl)acridin-9(10H)-one (16)

Compound **16** (0.09 g, 0.24 mmol) was synthesized using compound **10** (0.1 g, 0.35 mmol) according to the synthetic procedure C as a yellow solid in a yield of 67%, mp 100 °C; IR (KBr, cm^{-1}): 1592 (C=O), 3342 (OH); UV (ethanol + HEPES buffer) λ_{max} (ϵ) 237 (11,270), 254 (20,870), 401 (6550); ^1H NMR (300 MHz, CDCl_3) δ 1.07 (d, $J = 6.8$ Hz, 6H, $2 \times \text{CH}_3$), 1.10 (d, $J = 6.6$ Hz, 6H, $2 \times \text{CH}_3$), 2.63 (dd, 1H, $^2J = 13.6$ Hz, $^3J = 9.4$ Hz, 13-H), 2.79 (dd, 1H, $^2J = 13.8$ Hz, $^3J = 4.0$ Hz, 13-H), 3.07–3.16 (m, 2H, NCH), 4.19–4.26 (m, 1H, 12-H), 4.42 (dd, 1H, $^2J = 16.0$ Hz, $^3J = 3.4$ Hz, 11-H), 4.54 (dd, 1H, $^2J = 16.0$ Hz, $^3J = 7.3$ Hz, 11-H), 7.22–7.33 (m, 2H, ArH), 7.69–7.75 (m, 3H, ArH), 8.52 (t, 1H, $J = 1.0$ Hz, ArH), 8.59 (t, 1H, $J = 0.9$ Hz, ArH); ^{13}C NMR (normal/DEPT-135): δ 19.89 (+ve CH_3), 23.06 (+ve, CH_3), 45.06 (–ve, CH_2), 47.58 (–ve, CH_2), 50.33 (+ve, CH), 50.79 (+ve, CH), 66.63 (+ve, C-12), 115.12 (+ve, ArCH), 115.48 (+ve, ArCH), 118.18 (+ve, ArCH), 120.32 (+ve, ArCH), 121.33 (absent, ArC), 122.39 (+ve, ArCH), 178.09 (C=O); MS (FAB) 386, 388 (3:1) (M^+). Anal. Calcd for $\text{C}_{22}\text{H}_{27}\text{ClN}_2\text{O}_2$: C, 68.29; H, 7.03; N, 7.24. Found: C, 68.27; H, 7.06; N, 7.28.

4.4.9. P-gp interaction studies

Stock solutions of compounds **3–8** and **11–16** were prepared at 10^{-2} M concentration and diluted to three concentrations 0.5 μM , 5 μM , and 50 μM . Further dilutions take place during the assay and the final concentrations become 0.05 μM , 0.5 μM , and 5 μM . Each well of 96-well plate was dispensed with 80 μL of enzymatic buffer, 20 μL of PK/LDH solution, 10 μL of PEP solution and 10 μL of NADH solution. Additionally, 60 μL of enzymatic buffer was added to the total activity well; 30 μL of non-specific ATPase inhibitor solution and 30 μL enzymatic buffer was added to basal activity well; 30 μL non-specific ATPase inhibitor solution, 10 μL each of verapamil, progesterone, vinblastine, and 20 μL enzymatic buffer was added to the reference wells and 30 μL non-specific ATPase inhibitor solution, 30 μL enzymatic buffer to non-specific activity well. Blank well contains 200 μL of enzymatic buffer. The plate was incubated for 30 min at 37 °C. 10 μL of enzymatic buffer was added to non-specific activity wells and 10 μL of membrane vesicles were added to all other wells except blank well. Plate was incubated for 5 min at 37 °C, dispensed 20 μL of compound at each concentration and again incubated for 5 min at 37 °C. Finally, 10 μL of MgATP was added to each well except blank well and plate was incubated for 20 min at 37 °C. Plate was read at 340 nm followed by incubation and again reading after 20 min.

4.4.10. Interactions of compounds 11–16 with ATP

Stock solutions of compounds **11–16** were prepared at 10^{-3} M concentration by dissolving the compound in 2–3 drops of ethanol and making final volume up to 10 ml in HEPES Buffer (10^{-2} M, pH 7.2). This solution is further diluted to 50 μM concentration in HEPES buffer. Stock solution (10^{-2} M) of ATP was prepared by dissolving NaATP in HEPES Buffer. Taking the ligand concentration constant, upon addition of increasing concentration of ATP there is decrease in absorbance up to the addition of 3 equiv of ATP solution. The binding constants of compounds **11–16** with ATP were calculated using Benesi–Hildebrand equation³⁴ (Supplementary data).

4.4.11. Interactions of compounds 3–8 and 11–16 with Mg^{2+}

Stock solutions of compounds **3–8** and **11–16** (10^{-3} M) were prepared by dissolving the compounds **3–8** and **11–16** in 2–3 drops

of ethanol and making final volume up to 10 ml in HEPES buffer (10^{-2} M, pH 7.2). The solutions of compounds were further diluted to 10^{-4} M concentration in HEPES buffer. Upon titration with increasing concentration of Mg^{2+} by taking ligand concentration constant, regular increase, decrease was observed up to 0.5 equiv of Mg^{2+} . The binding constants of the compounds **3–8** and **11–16** were calculated using Benesi–Hildebrand equation.

4.4.12. MIC₈₀ assays

MIC₈₀ values for the compounds were determined using broth dilution method. Briefly, the *Candida* CAI4 strain was streaked on a YEPD plate and incubated at 30 °C for 24 h. In a 96-well flat bottom microtitre plate, the compounds were serially diluted twofold in YEPD medium upto the 10th column. The 11th and 12th columns were our control lanes to monitor for contamination during the experiment and as growth control to determine MIC₈₀ values, respectively. Similarly, a volume of solvent corresponding to the volume of the compound used for dilution was also diluted to see the effect of the solvent on the growth of the cells. The cells were picked from the YEPD plate, and suspended in 0.9% saline to obtain an O.D._{600 nm} equal to 0.1. This cell suspension was further diluted 100-fold in YEPD medium and 100 µL of this cell suspension was added to all the wells, except 11th column. The plates were incubated at 30 °C for 48 h and O.D._{600 nm} was monitored using ELISA plate reader. MIC₈₀ values were calculated by determining the concentration of the compound which resulted in an inhibition of cell growth by 80% as compared to the cell growth in the absence of the compound.

4.4.13. Spot assays

Plate assays were performed for the compound **3**. YEPD-Agar plates with the compound, and other toxins (Congo red, calcofluor white) were made. The solvent control plates were made by taking the same volume of solvent (MeOH/DMSO 1:1), as the volume of the compound used in the plates. One control plate was also made with YEPD alone. The primary culture was grown by taking CAI4 streak in 10 ml YEPD medium and growing for 16 h at 30 °C. Secondary culture was grown in 10 ml of YEPD with 4% inoculum from the primary culture, and grown at 30 °C for 5 h. O.D._{600 nm} was observed for the secondary culture, and diluted to obtain an O.D. of 0.1. This cell suspension was further serially diluted fivefold in 0.9% saline and 5 µL of these cell suspension, corresponding to 10^5 , 10^4 , 10^3 , 10^2 , 10^1 , 10^0 cells, were spotted on the plates. The plates were incubated at 30 °C for 48 h and then checked for growth.

4.4.14. Rhodamine 6G (R6G) influx/efflux assay (screening for MDR modulation)

R6G influx and efflux in the CAI4 cells was monitored in the presence and the absence of compound **3**. 10 ml of CAI4 primary culture was grown in YEPD medium at 30 °C for 24 h. Secondary culture was grown in 600 ml YEPD with 2% inoculum from primary culture, and grown at 30 °C for around 5 h. The cells were then pelleted at 4000 rpm and washed twice with PBS. The cell pellet was divided into six sets, 2% cell suspension of each was made in PBS with 2 mM 2-deoxyglucose and then kept on a rocker for 2 h. After 2 h 800 µg/ml of compound **3** was added to two of the sets while 375 µL of solvent (methanol/DMSO 1:1) was added to the solvent control sets. 10 µM/ml of R6G was added to each set. 700 µL aliquots were taken from each set at this time point (considered as 0 min), and then kept back at rocker. Aliquots were taken out at different time points, spun at 2000 rpm for 2 min and the supernatant was transferred into a fresh Eppendorf. The amount of R6G in the medium was monitored by measuring O.D._{527 nm}. After 3 h of incubation with R6G, the cells were again pelleted at 2000 rpm and washed twice with PBS. The cell pellets were further divided

into two sets each. PBS was added to one of the sets while 2% glucose in PBS was added to the other set, to obtain a 2% cell suspension. The cell suspensions were then kept back at rocker and aliquots were taken out at different time points, up to 3 h. The aliquots were spun at 2000 rpm for 2 min and the supernatant was used for monitoring the amount of drug effluxed out from the cells. The fluorescence intensity was monitored on a Cary-Varian spectrofluorimeter using excitation wavelength of 529 nm and emission wavelength of 553 nm (5 nm excitation and emission slit widths).

Acknowledgments

The financial assistance from DST, New Delhi is gratefully acknowledged. J.K. thanks UGC, New Delhi for fellowship. CDRI, Lucknow is acknowledged for recording mass spectra.

Supplementary data

Supplementary data (Job plots, Hildebrand equation, ¹H NMR spectra, physico-chemical parameters, docking complex and energy minimized compound– Mg^{2+} complexes) associated with this article can be found, in the online version, at [doi:10.1016/j.bmc.2010.05.003](https://doi.org/10.1016/j.bmc.2010.05.003).

References and notes

- Teodori, E.; Dei, S.; Scapecchi, S.; Gualtieri, F. *Il Farmaco* **2002**, *57*, 385.
- Dantzig, A. H.; Law, K. L.; Cao, J.; Starling, J. J. *Curr. Med. Chem.* **2001**, *8*, 39.
- Veen, H. W. V.; Higgins, C. F.; Konings, W. N. *Res. Microbiol.* **2001**, *152*, 365.
- Eckford, P. D. W.; Sharom, F. J. *Chem. Rev.* **2009**, *109*, 2989.
- Aller, S. G.; Yu, J.; Ward, A.; Weng, Y.; Chittaboina, S.; Zhuo, R.; Harrell, P. M.; Trinh, Y. T.; Zhang, Q.; Urbatsch, E. L.; Chang, G. *Science* **2009**, *323*, 1718.
- Lamping, E.; Monk, B. C.; Nimi, K.; Holmes, A. R.; Tsao, S.; Tanabe, K.; Nimi, M.; Uehara, Y.; Cannon, R. D. *Eukaryot. Cell* **2007**, *6*, 1150.
- Prasad, R.; Panwar, S. *Curr. Sci.* **2004**, *86*, 62.
- Kawase, M.; Motohashi, N. *Curr. Drug Targets* **2003**, *4*, 31.
- Pina-Vaz, C. I.; Rodrigues, A. G.; Costa-de-Oliveira, S.; Ricardo, E.; Mardh, P.-A. *J. Antimicrob. Chemother.* **2005**, *56*, 678.
- Shukla, S.; Sauna, Z. E.; Prasad, R.; Ambudkar, S. V. *Biochem. Biophys. Res. Commun.* **2004**, *322*, 520.
- Lehninger, A. L.; Nelson, D. L.; Cox, M. M. In: *Principles of Biochemistry*, 2nd ed., 1992, p 374, CBS ISBN 81-239-0295-6.
- Gomez-Puyou, A.; Ayala, G.; Muller, U.; Gomez-Puyou, T. De. *J. Biol. Chem.* **1983**, *258*, 13673.
- Phillips, R. C.; George, S. J. P.; Rutman, R. J. *J. Am. Chem. Soc.* **1966**, *88*, 2631.
- Singh, P.; Kaur, J.; Kaur, P.; Kaur, S. *Bioorg. Med. Chem.* **2009**, *17*, 2423.
- Belmont, P.; Bosson, J.; Godet, T.; Tiano, M. *Anticancer Agents Med. Chem.* **2007**, *7*, 139.
- Goodell, J. R.; Ougolkov, A. R.; Hiasa, H.; Kaur, H.; Remmel, R.; Billadeau, D. D.; Ferguson, D. M. *J. Med. Chem.* **2008**, *51*, 179.
- Kawai, S.; Tomono, Y.; Katase, E.; Ogawa, K.; Yano, M.; Takemura, Y.; Ju-ichi, M.; Ito, C.; Furukawa, H. *J. Nat. Prod.* **1999**, *62*, 587.
- Winter, R. W.; Kelly, J. X.; Smilstein, M. J.; Dodean, R.; Bagby, G. C.; Rathbun, R. K.; Levin, J. I.; Hinrichs, D.; Riscoe, M. K. *Exp. Parasitol.* **2006**, *114*, 47.
- Dheyongera, J. P.; Geldenhuy, W. J.; Dekker, T. G.; Matsabisa, M. G.; Van der Schyf, C. J. *Bioorg. Med. Chem.* **2005**, *13*, 1653.
- Di Giorgio, C.; Shimi, K.; Boyer, G.; Delmas, F.; Galy, J.-P. *Eur. J. Med. Chem.* **2007**, *42*, 1277.
- Goodell, J. R.; Madhok, A. A.; Hiasa, H.; Ferguson, D. M. *Bioorg. Med. Chem.* **2006**, *14*, 5467.
- Gopinath, V. S.; Thimmaiah, P.; Thimmaiah, K. N. *Bioorg. Med. Chem.* **2008**, *16*, 474.
- Boumndjel, A.; Macalou, S.; Ahmed-Belkacem, A.; Blanc, M.; Di Pietro, A. *Bioorg. Med. Chem.* **2007**, *15*, 2892.
- Singh, P.; Kaur, J.; Yadav, B.; Komath, S. S. *Bioorg. Med. Chem.* **2009**, *17*, 3973.
- Ullmann, F. *Ber.* **1903**, *36*, 2383.
- Yamamoto, T.; Kurata, Y. *Can. J. Chem.* **1983**, *61*, 86.
- Tercio, J.; Ferreira, B.; Catani, V.; Comassetto, J. V. *Synthesis* **1987**, *2*, 149.
- Sabitha, G.; Reddy, B. V. S.; Abraham, S.; Yadav, J. S. *Green Chem.* **1999**, *1*, 251.
- Mojtahedi, M. M.; Saidi, M. R.; Bolourtchian, M. *J. Chem. Res., Synop.* **1999**, *2*, 128.
- 'P-gp–Drug Interaction Assay kit' was purchased from CaymanChemicals, Cat no. 789201.
- Neelakandan, P. P.; Hariharan, M.; Ramaiah, D. *Org. Lett.* **2005**, *7*, 5765.
- Talibi, D.; Raymond, M. J. *Bacteriol.* **1999**, *181*, 231.
- ArgusLab, Thompson, M. A., Planaria Software LLC, Seattle, WA 98155.
- Hildebrand, J. H.; Benesi, H. A. *J. Am. Chem. Soc.* **1949**, *71*, 2703.